

CREEP AND SHRINKAGE OF A HIGH STRENGTH CONCRETE MIXTURE

Brad Townsend, Hayes, Seay, Mattern and Mattern, Roanoke, VA
Richard Weyers, PhD, PE, Dept. of Civil Engineering, Virginia Tech

ABSTRACT

Test beams for the Pinner's Point Bridge were fabricated by Bayshore Concrete Products Corp., in Cape Charles, VA. The beams were cast using high strength concrete mixtures with specified 28-day compressive strengths of 8,000 psi and 10,000 psi. Laboratory creep and shrinkage testing was conducted on specimens prepared with similar materials, mixture proportions, and curing conditions to those used at Bayshore. Strains were measured using a Whittemore gage. Vibrating wire gages (VWGs) were cast in the center of four cylinders which also had Whittemore gage points. The Whittemore and VWG elastic and creep strains were similar, while the VWGs recorded significantly less shrinkage. The measured creep and shrinkage strains were compared to seven current prediction models to determine the most accurate predictor. The ACI 209 modified by Huo was most accurate in predicting time-dependent strains.

Keywords: creep, shrinkage, high strength concrete, prediction models, vibrating wire gages

INTRODUCTION

The use of high strength concrete (HSC) has been steadily increasing, and today it is a very popular construction material. Concrete having a 28-day compressive strength of at least 6000 psi is normally considered high strength.¹ High compressive strengths are achieved by using a low water-to-cementitious materials ratio, requiring the use of water-reducing admixtures to provide adequate workability. High strength concrete offers significant economic advantages over conventional normal strength concrete (NSC) because more slender members can be designed, resulting in reduced material and transportation costs. As structural components become more slender, deflection becomes a more crucial issue, making long-term creep and shrinkage deformations especially important in HSC structures.

All concrete structures undergo time-dependent deformations known as creep and shrinkage. Creep is defined as the deformation over time of a viscoelastic material, in excess of initial elastic strain, that results when a sustained stress is applied. Shrinkage is also a time-dependent deformation, but it occurs in the absence of any applied load. Therefore, the total strain of a concrete specimen at any time is the sum of its initial elastic strain, creep strain, and shrinkage strain.

Creep of concrete may be separated into two components: basic creep and drying creep. Basic creep occurs in a sealed condition, without any exchange of water between the concrete and its surroundings. Drying creep involves water movement to the surrounding environment. The creep experienced by the innermost region of a large concrete member is predominantly basic creep, since very little water is lost to the outside environment.

Shrinkage consists of three different mechanisms, known as drying shrinkage, autogenous shrinkage, and carbonation. Drying shrinkage occurs when excess water not consumed during hydration diffuses into the surrounding environment, resulting in a net volume loss. Autogenous shrinkage is the water loss due to continued hydration of the cement. Carbonation shrinkage is the process by which CO_2 in the atmosphere reacts with $\text{Ca}(\text{OH})_2$ in the cement paste, in the presence of moisture.

The main purpose of this study is to observe the time-dependent deformation of a high strength concrete mixture used in prestressed bridge girders for the Pinner's Point Bridge. This project consists of creep and shrinkage testing under laboratory conditions. In a related project, several test beams at Bayshore Concrete Products Corporation were instrumented in order to study prestress losses. Results from this study may be compared to the time-dependent deformations measured in the field.

Another objective is to compare observed creep and shrinkage deformations with seven current prediction models and determine which model most accurately predicts creep and shrinkage strains for this mixture.

The materials and mixture proportions used in producing laboratory specimens matched those used in the field. The test variables were specimen size and curing method.

Accelerated curing was used for two batches, using a match cure system to replicate the time-temperature profile of the test beams during steam curing. The other two standard test batches were moist cured for seven days.

METHODS AND MATERIALS

The test matrix for this study is presented in Table 1.

Table 1 HSC Test Matrix

Curing Method	Batches	Age at Loading	Specimens/Batch
Standard	HSC8-3A HSC8-4A	7 days	8 Compressive Strength 4 Tensile Strength 1 Modulus 3 Shrinkage 3 Creep 3 Shrinkage Prisms
Accelerated	HSC8-1A HSC8-2A	1 day	5 Compressive Strength 2 Tensile Strength 1 Modulus 4 Shrinkage Cylinders 4 Creep Cylinders

Batch mixing was conducted in accordance with ASTM C192.² Mixture proportions were determined based on the 55.2 MPa (8000 psi) mix design used in the test beams at Bayshore. These proportions are presented in Table 2. For some of the batches, additional HRWR was added in order to achieve the desired slump.

Table 2 Bayshore Mixture Proportions

Materials	SSD weights, lb/yd³
Portland Cement	510
GGBFS	340
Course Aggregate	1950
Fine Aggregate	988
Water	252
AEA	15 oz/yd ³
WR	27 oz/yd ³
HRWR	175 oz/yd ³
Corrosion Inhibitor	4.0 gal/yd ³

Tables 3 and 4 present the laboratory fresh concrete properties for the accelerated cure and standard cure batches, respectively. Table 3 also includes the prestressed beam fresh concrete properties as reported by Bayshore and VDOT specifications.

Table 3 Accelerated Cure Laboratory and Beam Fresh Concrete Properties

Properties	HSC8-1A	HSC8-2A	Bayshore	VDOT Specs.
Slump, in.	6	6	8	0-7
Air Content, %	5.6	4.4	6.2	3-6
Temperature, °F	76	78	77	40-90
Unit Weight, pcf	154	155	----	----
Yield	1.02	1.03	----	----
w/cm ratio	0.30	0.30	~ 0.33	< 0.4
Curing Method	Match Cure	Match Cure	Steam	N/A

Table 4 Standard Cure Laboratory Fresh Concrete Properties

Properties	HSC8-3A	HSC8-4A
Slump, in.	8.5	4.5
Air Content, %	3.5	3.5
Temperature, °F	78	75
Unit Weight, pcf	159	159
Yield	1.05	1.05
w/cm ratio	0.30	0.30

MATERIALS

The materials used in fabricating the laboratory concrete specimens were obtained from Bayshore, in order to match the materials in the test beams.

The coarse aggregate is a #67 crushed stone from Garrisonville, VA, and the fine aggregate is a natural sand from King George County, VA. Cementitious materials consist of Type II Portland Cement and a ground granulated blast furnace slag (GGBFS). The GGBFS is a grade 120. The admixtures were air entrainment, water reducer, a polycarboxylate based high-range water reducer, and a calcium nitrite corrosion inhibitor. The corrosion inhibitor also acts as an accelerator.

CURING

For the two accelerated cure batches, cylindrical specimens were cast in 4 in. x 8 in. molds whose curing temperatures were controlled by the match cure system. A 22-hour heated curing regimen was used to simulate steam curing of the test girders at Bayshore. The temperature profile of the test girders during steam curing was recorded using embedded thermocouples. This profile was entered into the match cure system, so that the test specimens would experience the same curing temperatures as the test girders. In order to

maintain a moist environment, wet burlap and plastic sheeting were placed over the molds during curing.

The cylindrical standard cure creep and shrinkage specimens were cast in 6 in. x 12 in. steel molds, while the cylindrical strength and modulus specimens were cast in 4 in. x 8 in. plastic molds. Shrinkage prisms were cast in 3 in. x 3 in. x 11.25 in. steel rectangular molds. The test specimens were stored in a moist room for 7 days after casting, in accordance with the standard curing procedure of ASTM C192.²

CREEP TESTING

Creep testing was performed in accordance with ASTM C512.³ Because of equipment constraints, there were differences in test procedure between the standard cure and accelerated cure batches.

From each accelerated cure batch, four cylindrical creep and shrinkage specimens were cast. Holes were drilled in the cylinders and the gage points were attached using a five-minute epoxy. The gage points were spaced 6 in. apart for the accelerated cure specimens.

From each standard cure batch, three cylindrical creep and shrinkage specimens were cast, along with the strength and elastic modulus specimens. Brass inserts were cast into each creep and shrinkage cylinder, so that gage points could be attached after curing. Each cylinder has four gage points, with two on each diametrically opposite side, separated by 8 in.

Test specimens were sulfur-capped immediately after curing, in accordance with ASTM C617.⁴ Compressive strength was determined immediately after curing, and the creep, shrinkage, elastic modulus, and remaining strength specimens were placed in the controlled environment of 73.4 ± 3 °F and 50 ± 4 % relative humidity. The creep specimens were stacked in the loading frames and loaded to 30 % of their after cure compressive strength. The applied load was kept constant throughout the test. Within-batch deviations in stress were eliminated since all loaded specimens from a batch were placed in the same loading frame.

Creep and shrinkage measurements were taken on the schedule set forth in ASTM C512,³ using a Whittemore gage to measure changes in length between the gage points over time. The Whittemore gage reads lengths in increments of 0.0001 in., which equals 17 and 13 microstrain for the accelerated and standard cure specimens, respectively. Measurements were repeated four times on each side of the cylinder, so that each reading is an average of eight measurements.

Vibrating wire gages (VWG) identical to the ones used in the test girders were embedded in the center of two cylindrical creep and shrinkage specimens of accelerated batch 2A. Readings were taken at the same time increments as the Whittemore measurements, and the

two were compared in order to observe differences in creep and shrinkage behavior between the center of a concrete specimen and the outer surface

STRENGTH TESTING

Compressive and tensile strength tests were performed for each batch. Compressive tests followed ASTM C39,⁵ using 4 in. x 8 in. cylinders that were sulfur-capped and stored in the creep room after curing. For the standard cure batches, compressive tests on two specimens were performed at 7, 28, 56, and 90 days after casting. The match cure system limited the number of accelerated cure specimens that could be made, so compressive tests were performed at 1, 7, and 28 days after casting.

RESULTS

COMPRESSIVE STRENGTH

Figure 1 presents the HSC laboratory compressive strength results for accelerated batches 1A and 2A, as well as field results from Bayshore. Each one-day laboratory result represents an average of two measurements, and the others represent single measurements. Each result from Bayshore is an average of three measurements. The specified 28-day compressive strength (f'_c) of 8000 psi and release strength (f'_{ci}) of 6400 psi are presented for comparison.

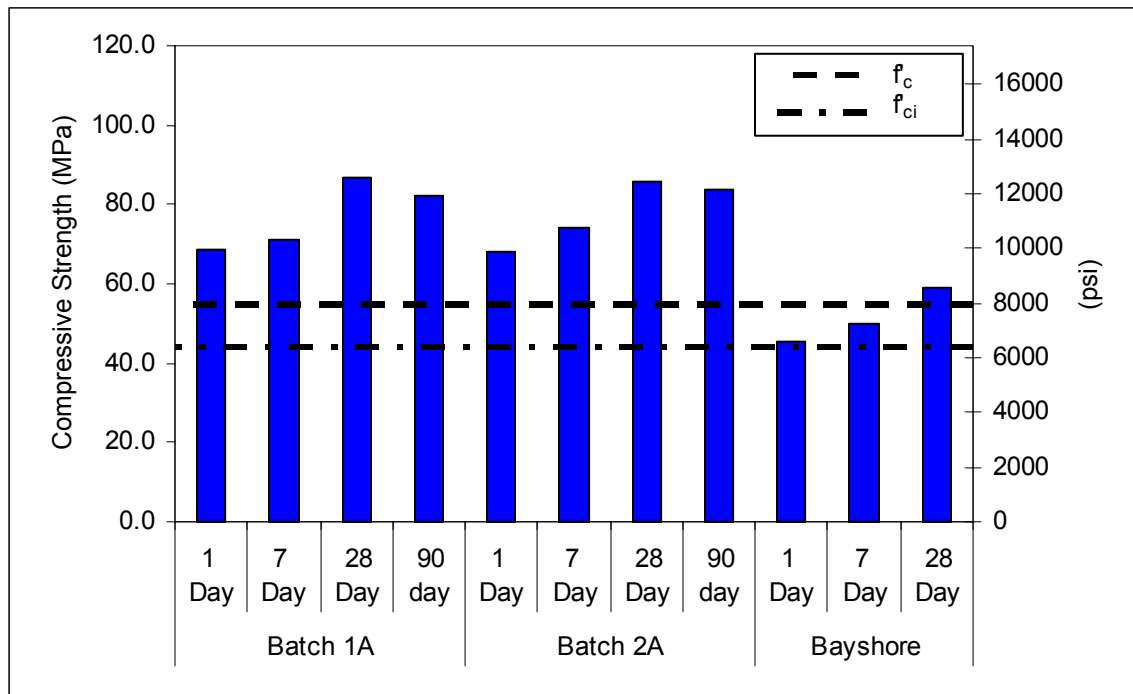


Fig. 1 Accelerated Cure Compressive Strengths

As seen in Figure 1, the Bayshore compressive strengths were 30 percent lower than the laboratory accelerated cure strengths. This disparity is due in part to differences in the amounts of water in the concrete mixtures. The aggregate for the laboratory mixtures was dried before mixing, whereas the aggregate in Bayshore's mixtures was likely in SSD condition. Aggregate absorption was not accounted for in the laboratory mixtures, resulting in a w/cm ratio of 0.30. The w/cm ratio should have been 0.33 with the aggregate in SSD condition. According to charts found in "High Performance Concrete: Properties and Applications," a decrease in w/cm ratio from 0.33 to 0.30 would cause a compressive strength increase of at most 2000 psi, which is half of the observed strength difference.¹ The Bayshore concrete also had a higher air content than the laboratory mixtures (see table 3), but the differences in air content and w/cm ratio do not fully explain the strength differences. A possible explanation is that the Bayshore mixture contained more water than the amount specified in the mix design. The fact that the Bayshore mixture had a higher air content than

the laboratory mixtures supports this explanation in that a higher water content increases fluidity and air content of a mixture.

Figure 2 presents the HSC laboratory compressive strength results for standard cure batches 3A and 4A. Each result represents an average of two compressive strength measurements. The specified 28-day compressive strength (f'_c) of 8000 psi and release strength (f'_{ci}) of 6400 psi are presented for comparison.

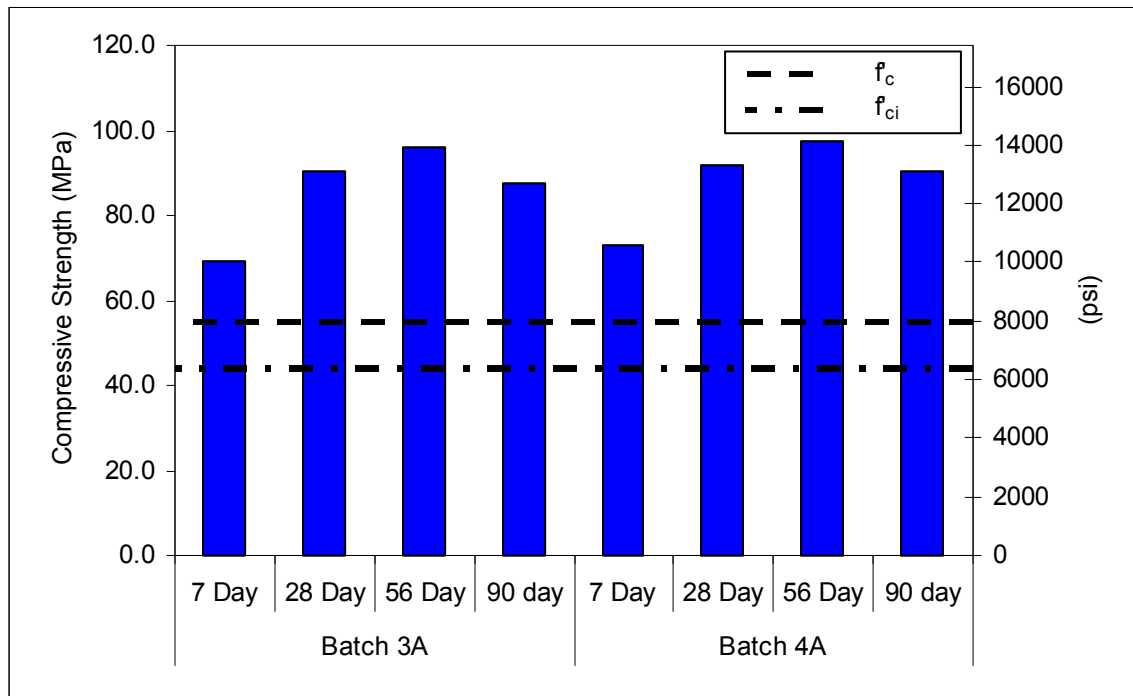


Fig. 2 Standard Cure Compressive Strengths

The average seven-day strengths for the two curing methods were similar, but the standard cure batches had significantly higher strength gain with time. This is because the accelerated curing procedure consumes more water and creates a more porous hydrated cement matrix than standard curing. The standard cure specimens contained more excess water after curing, which allowed for continued hydration and thus densification of the cement matrix. The use of accelerated curing allows for rapid initial strength gain, but significantly decreases the potential for continued strength gain after curing.

EXPERIMENTAL STRAINS

Figures 3 and 4 present the HSC experimental total strain, shrinkage, and creep measurements for the accelerated cure and standard cure batches. Measurements were taken daily for a week after loading, then weekly thereafter, but some measurements are not shown in the figures for clarity. Each accelerated cure curve represents an average of 8 specimens, and each standard cure curve represents an average of 6 specimens. Each creep curve

represents an average of 8 (accelerated cure) or 6 (standard cure) pairs of loaded and unloaded specimens.

The figures also present 95 percent confidence intervals for each data point. The 95 percent confidence interval is the range in which 95 percent of the population measurements can be expected to be within.

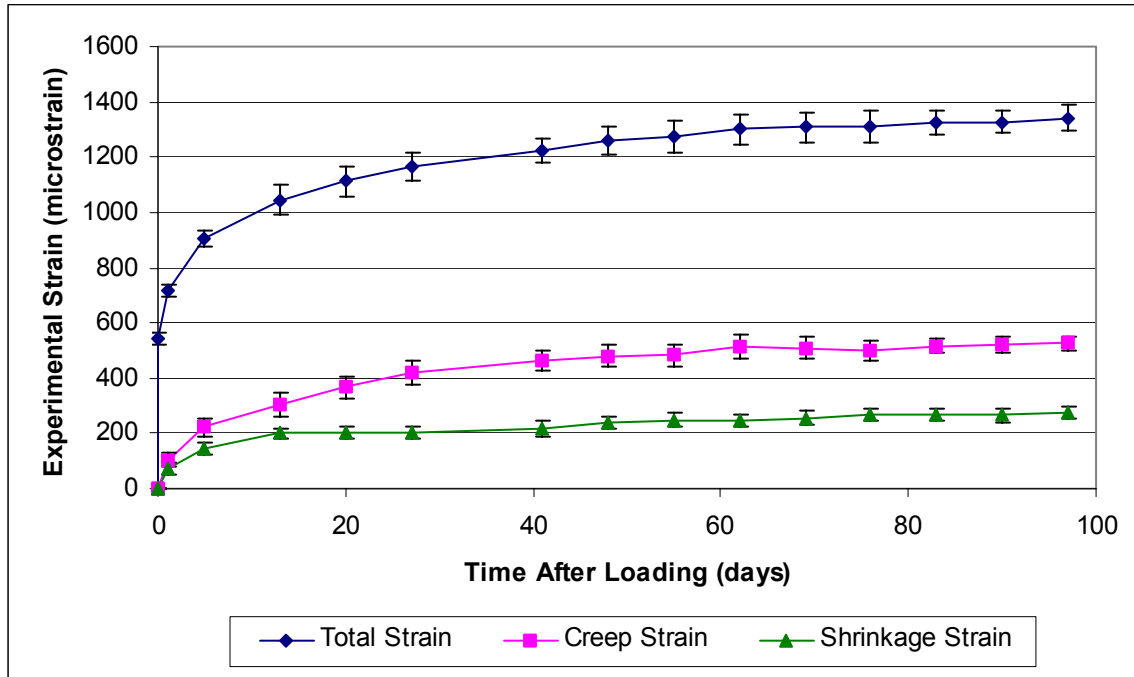


Fig. 3 Accelerated Cure Experimental Strains

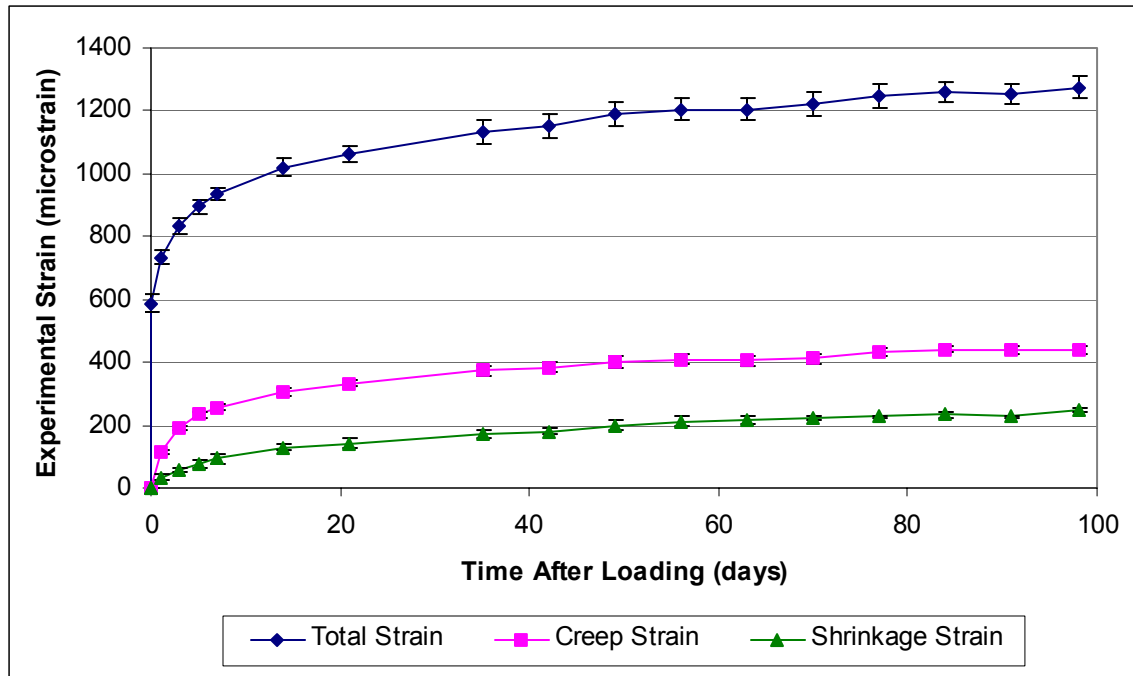


Fig. 4 Standard Cure Experimental Strains

A noticeable difference is observed between the accelerated cure and standard cure curves in that the standard cure curves have much smaller 95 percent confidence intervals. This indicates that the accelerated cure batches had much more within-batch variation, which is likely a result of the following factors:

- Curing conditions. More variability is inherent with accelerated curing than standard curing. This is corroborated by Vincent's research.⁶
- Gage lengths. The standard cure specimens have an 8 in. gage length, while the accelerated cure gage length is 6 in. Equal length measurement errors result in 33 percent more strain variation for the smaller gage length than for the larger one.
- Learning error. The standard cure batches were tested last, so the standard cure results probably contain less measurement error than the accelerated cure results

EXPERIMENTAL STRAIN RELATIONSHIPS

Accelerated Cure vs. Standard Cure

Accelerated and standard cure specimens can be expected to behave differently over time because of differences in specimen size, curing method, and compressive strength. Larger specimens generally have less drying creep and shrinkage, especially early on, because it is more difficult for water to move from the center of the specimen to the outside surface. Accelerated curing forms larger hydration products than standard curing. As a result, standard cure specimens have a denser concrete matrix that is more resistant to water movement, thus reducing drying creep and shrinkage. The standard cure specimens had greater compressive strength gain with time than the accelerated cure specimens. As a result,

the standard cure creep specimens were loaded to a smaller fraction of their compressive strength at later ages, since the applied stress was kept constant for both curing methods. The following figures do not include any adjustment factors for size or compressive strength. The accelerated cure and standard cure data sets are averages of eight and six specimens, respectively.

The relationship between average accelerated cure and standard cure total strains is presented in Figure 5. The two data sets are nearly equivalent early on, but the accelerated cure strains are higher at later ages.

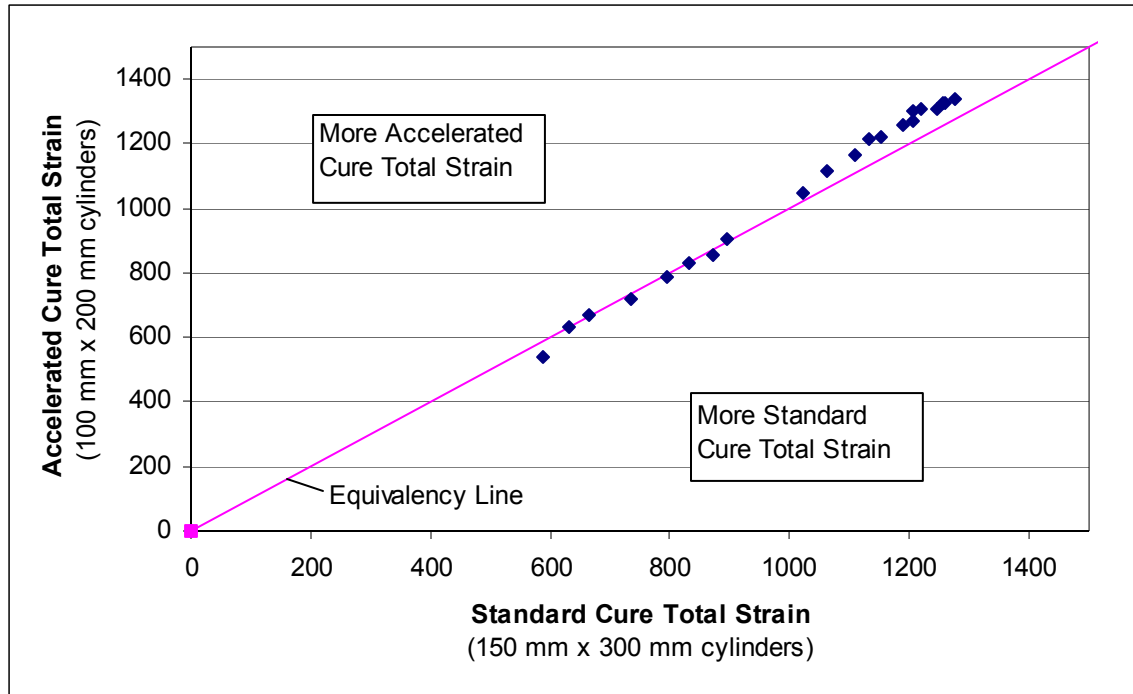


Fig. 5 Accelerated Cure vs. Standard Cure Total Strain (microstrain)

The relationship between average accelerated cure and standard cure creep strains is presented in Figure 6. The accelerated cure creep strain is significantly higher at later ages. The smaller specimen size resulted in higher drying creep. In addition, the accelerated cure specimens had a less dense cement matrix and less strength gain with time.

The relationship between average accelerated cure and standard cure shrinkage strains is presented in Figure 7. Shrinkage strain is higher for the accelerated cure specimens due to smaller specimen size and a less dense concrete matrix.

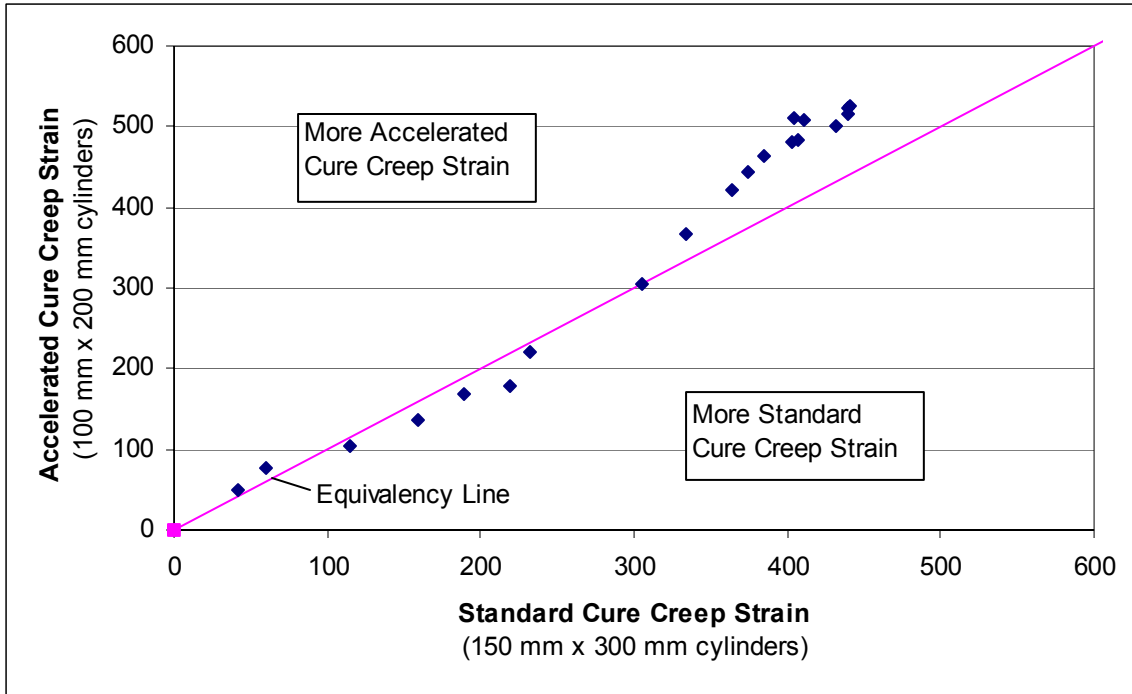


Fig. 6 Accelerated Cure vs. Standard Cure Creep (microstrain)

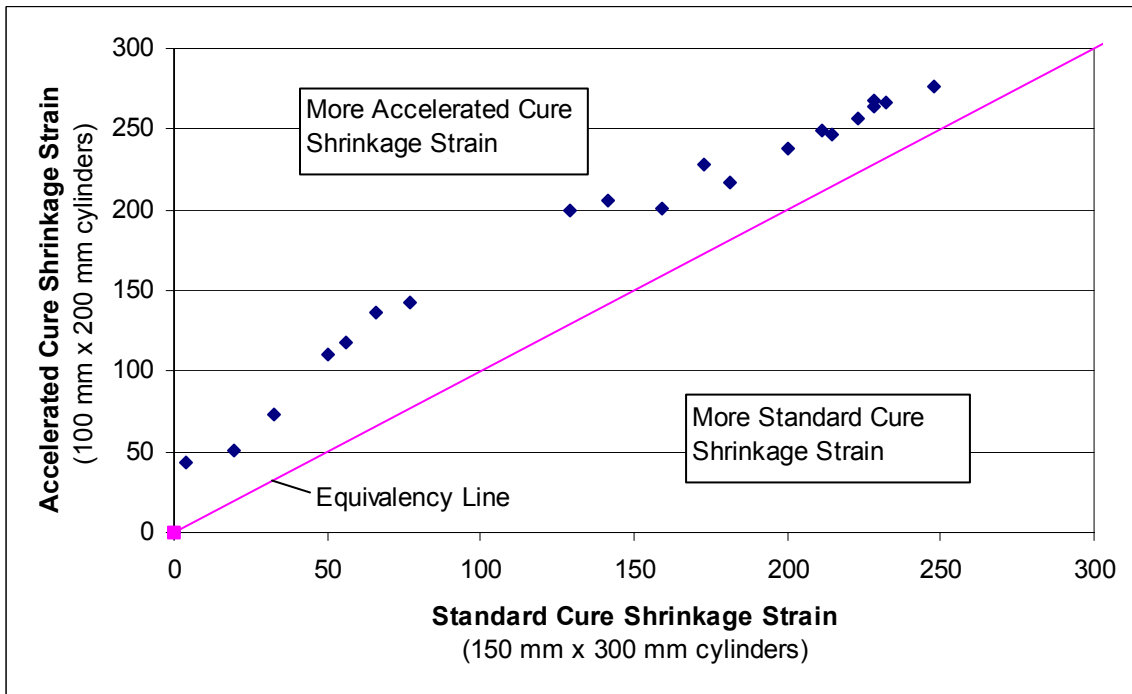


Fig. 7 Accelerated Cure vs. Standard Cure Shrinkage (microstrain)

Field vs. Laboratory

Figure 8 presents the relationship between time-dependent strains measured on test girders at Bayshore and those measured in the laboratory. The strain measurements are divided by applied stress, which is not a constant for the two data sets. The field stress is calculated as the initial elastic stress minus estimated prestress losses over time. The field data was obtained from Chris Waldron, and represents the average total strain at the center of prestressing for three test girders.⁷ The laboratory data represents the average total strain of eight accelerated cure specimens. The data is not adjusted for parameters such as specimen size, compressive strength, and relative humidity.

The laboratory specimens had significantly higher time-dependent deformations than the test girders. This is to be expected due to the following factors:

- Size effects: The field measurements were taken in the center of a large girder, where drying creep and shrinkage are limited.
- Ambient conditions: The average relative humidity at Bayshore is over 70 percent, compared to the laboratory relative humidity of 50 percent. Relative humidity has a significant effect on drying creep and shrinkage.

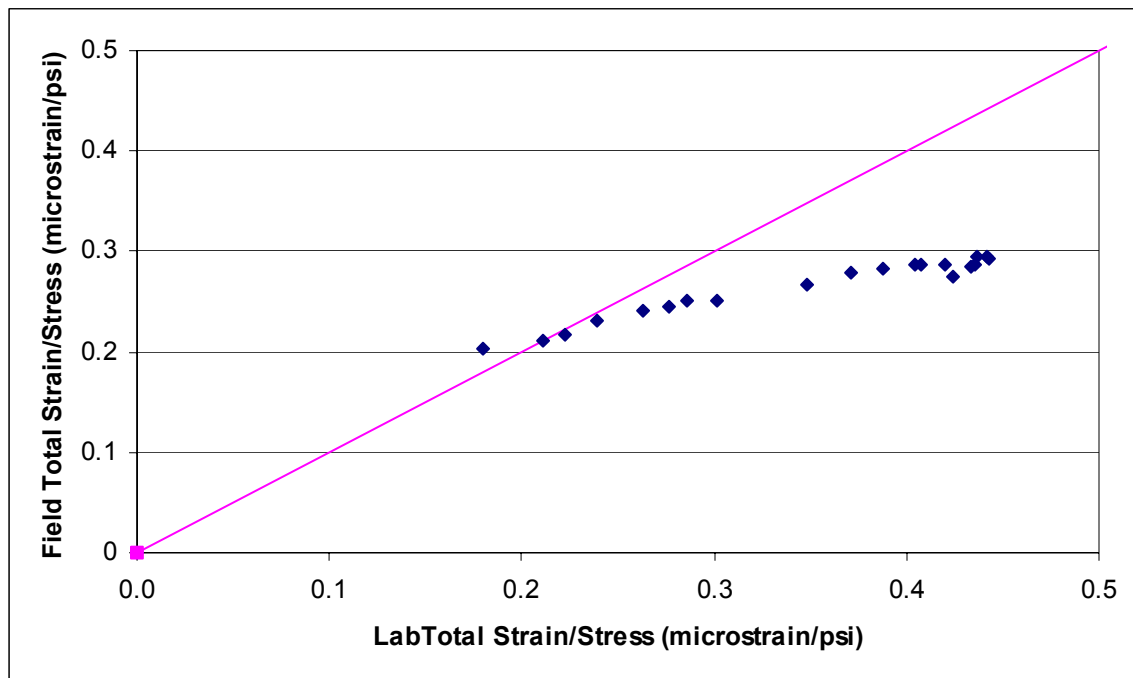


Fig. 8 Field vs. Laboratory Accelerated Cure Total Strains

Vibrating Wire Gage vs. Whittemore Gage

Figures 9 and 10 present strains measured using vibrating wire gages (VWG) and Whittemore gages. Each Whittemore measurement is an average of measurements taken on two diametrically opposite sides of the cylinder. Cylinder 2A-2 is a loaded creep specimen, while cylinder 2A-6 is an unloaded shrinkage specimen. For the loaded specimen, there is a general agreement between the strains measured using the two methods, with the VWG strains slightly lower than the Whittemore strains. The unloaded specimen had significantly less VWG strain over time than Whittemore strain. These observations indicate that shrinkage strain is higher at the surface of the specimen than in the middle, but creep and elastic strains are similar at the two locations.

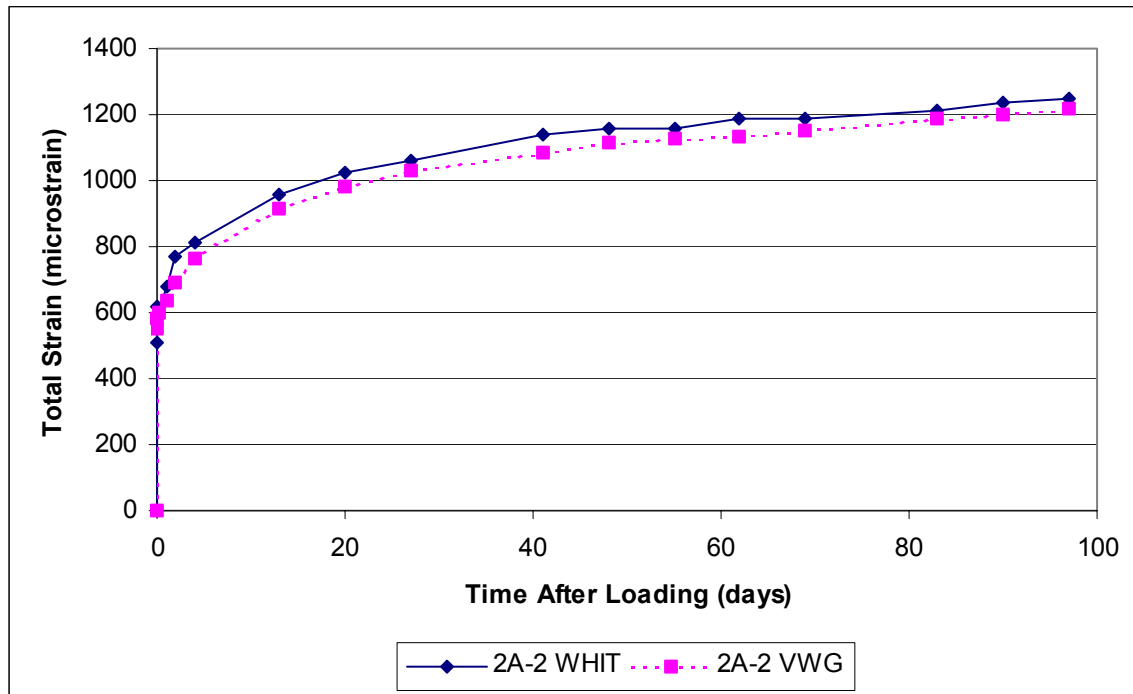


Fig. 9 Cylinder 2A-2 Whittemore and VWG Total Strains

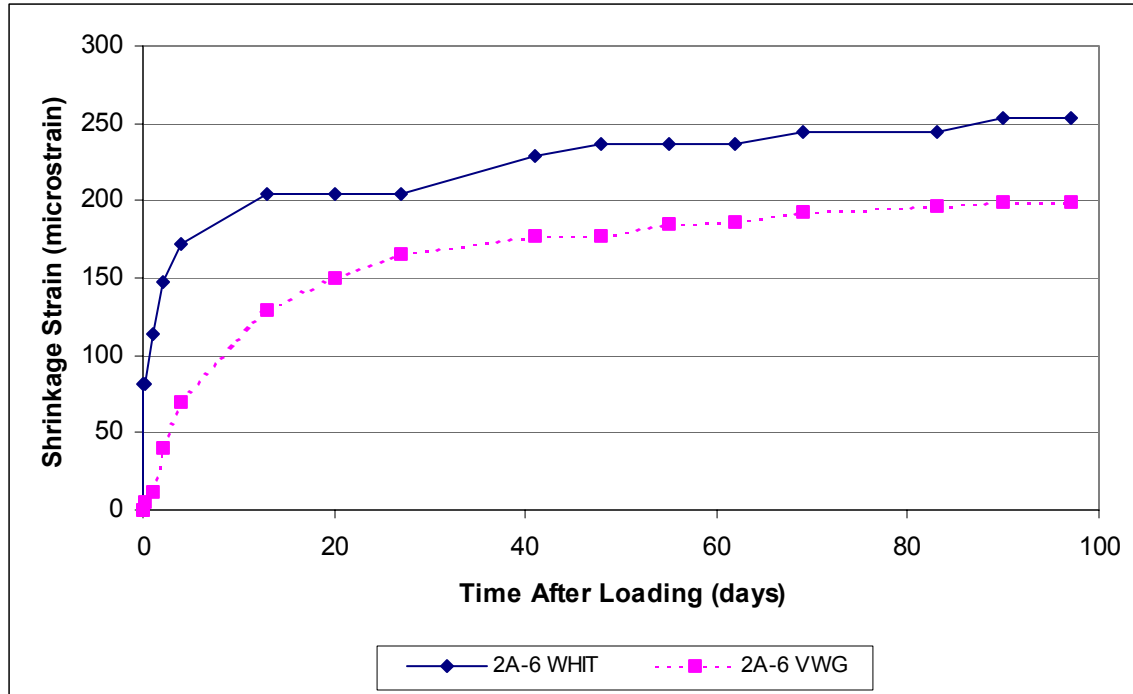


Fig. 10 Cylinder 2A-6 Whittemore and VWG Shrinkage Strains

PREDICTION MODELS

The predicted strains were calculated using measured compressive strengths and elastic strains. The predicted time-dependent strains were added to the measured initial elastic strains. The following models were considered:

- ACI 209R-92 (ACI 209)⁸
- ACI 209R-92, modified by Huo (ACI 209 Modified)⁹
- Comite Euro-International Du Beton Model Code 1990 (CEB 90)¹⁰
- AASHTO-LRFD Specification (AASHTO-LRFD)¹¹
- Gardner and Lockman's GL2000 Model (GL2000)¹²
- Tadros' Revised AASHTO-LRFD (Tadros)¹³
- Bazant's B3 Model (B3)¹⁴

The equations for prestress loss due to creep and shrinkage in the AASHTO Standard Specification are based on the ACI 209 model.¹⁵

A residuals squared analysis of the total strain, creep, and shrinkage data was performed to determine which prediction model was the most accurate. A residual is defined as the algebraic difference between a predicted value and an experimental value. A negative residual indicates that a model is under predicting the experimental data, and a positive residual indicates the model is over predicting the experimental data. The following formula illustrates the procedure used to calculate the sum of residuals squared test statistic.

$$\text{Sum of Residuals Squared} = \sum_{t=t_i}^{t_f} [(Re_t)^2]$$

Where: t = time after loading
 t_i = initial time considered
 t_f = final time considered
 Re_t = Residual at time t

For example, if the sum of residuals squared is computed between 0 and 100 days after loading, then t_i = 0 and t_f = 100. By squaring the residual, this analysis method prevents negative and positive residuals from canceling each other out. The model with the lowest sum of residuals squared is the most accurate predictor.

Model Rankings

The prediction model rankings from the residuals squared analysis were summed to determine the best overall predictor. The accelerated cure and standard cure rankings are determined at 97 and 98 days after loading, respectively.

Table 5 presents the accelerated cure prediction model rankings. The ACI 209 Modified is the most accurate model for each type of strain.

Table 5 Accelerated Cure Prediction Model Rankings

	Total Strain	Creep	Shrinkage	Sum
ACI 209 Modified	1	1	1	3
Tadros	2	2	2	6
ACI 209	4	4	4	12
AASHTO-LRFD	3	3	7	13
B3	6	6	3	15
CEB MC-90	5	5	6	16
GL2000	7	7	5	19

Table 6 presents the standard cure prediction model rankings. The ACI 209 Modified is the best total strain and overall predictor. AASHTO-LRFD was the best predictor of creep strain, and B3 was the best predictor of shrinkage strain.

Table 6 Standard Cure Prediction Model Rankings

	Total Strain	Creep	Shrinkage	Sum
ACI 209 Modified	1	2	2	5
Tadros	2	3	4	9
AASHTO-LRFD	3	1	7	11
B3	6	6	1	13
CEB MC-90	4	5	5	14
ACI 209	5	4	6	15
GL2000	7	7	3	17

Applicability of Prediction Models

Creep and shrinkage behavior depend heavily on the compressive strength of a concrete mixture. High strength concrete has a more dense cement matrix and less free water than normal strength concrete, which are factors that limit the amount of time-dependent water movement within the cement matrix. For a prediction model to accurately predict creep and shrinkage strains for high strength concrete, it should include compressive strength as an important input parameter. Table 7 presents the applicability of each prediction model to high strength concrete.

Table 7 Prediction Model Compressive Strength Parameters

	f _c Limit, psi	Strength Adjustment Factor?	
		Creep	Shrinkage
ACI 209	none	no	no
ACI 209 Modified	none	yes	yes
CEB 90	13000	yes	yes
AASHTO-LRFD	none	yes	no
GL2000	10000	no	yes
Tadros	none	yes	yes
B3	10000	yes	yes

In this study, the models that did not include compressive strength as an input parameter greatly over predicted the experimental strains. In some cases, the models considered compressive strength for creep but not shrinkage, and vice versa (AASHTO-LRFD and GL2000).

The Bazant B3 and Gardner GL2000 prediction models are not expected to be accurate for the laboratory mixtures because the laboratory compressive strengths exceed the limits of applicability for each model. B3 considers compressive strength, but this parameter must be modified if the model is to be applied to concretes with compressive strengths of over 69.0 MPa (10000 psi). The GL2000 creep model does not consider compressive strength.

CONCLUSIONS

For Accelerated Cure Applications

1. The total strain of the HSC accelerated cure mixture loaded to 3000 psi was 1342 ± 49 microstrain at 97 days, at a 95 percent confidence level.
2. ACI 209 Modified by Huo is the most accurate predictor of total, creep, and shrinkage strain for the Bayshore HSC mixture loaded to 3000 psi.
3. The accelerated curing technique results in higher variability of time-dependent strains than standard curing.

4. Embedded Vibrating wire gages (VWG) may be used to measure laboratory time-dependent strains. VWG elastic and creep strain measurements are comparable to Whittemore Gage measurements. VWG drying creep and shrinkage strains are significantly lower than Whittemore shrinkage strains because more drying occurs at the outside surface of a specimen.

For Standard Cure Applications

1. The total strain of the HSC standard cure mixture loaded to 3000 psi was 1276 ± 38 microstrain at 98 days, at a 95 percent confidence level.
2. ACI 209 Modified by Huo is the best overall predictor and best predictor of total strain for the Bayshore HSC mixture loaded to 3000 psi.
3. AASHTO-LRFD is the best predictor of creep strain for the Bayshore HSC mixture loaded to 3000 psi.
4. B3 is the best predictor of cylinder shrinkage strain for the Bayshore HSC mixture, while GL2000 is the best predictor of prism shrinkage strain.

RECOMMENDATIONS

1. Creep and shrinkage models should contain modification factors for compressive strength. In this study, the models that contained such modification factors predicted much more accurately than those that did not consider compressive strength.
2. The AASHTO Standard Specification is used in Virginia, but it significantly over predicts prestress losses due to creep and shrinkage for high strength concrete. It should be updated by using a model that is applicable to high strength concrete.
3. Whenever possible, laboratory specimens should be cast in the field from the concrete batches being used in the test girders, so that the specimens are of identical material as the girders. This would eliminate significant discrepancies in material properties between the laboratory concrete and girder concrete.
4. Creep testing of sealed specimens could be useful in order to compare with creep strains inside a large bridge girder, where basic creep dominates.

REFERENCES

1. Shah, S. P. and Ahmad, S. H., "High Performance Concrete: Properties and Applications," McGraw-Hill, Inc., New York, 1994.
2. ASTM C192 *Making and Curing Test Specimens in the Laboratory*. American Society of Testing and Materials, Philadelphia, PA.
3. ASTM C512 *Creep of Concrete in Compression*. American Society of Testing and Materials, Philadelphia, PA.
4. ASTM C617 *Capping Cylindrical Concrete Specimens*. American Society of Testing and Materials, Philadelphia, PA.
5. ASTM C39 *Compressive Strength of Cylindrical Concrete Specimens*. American Society of Testing and Materials, Philadelphia, PA.
6. Vincent, Edward C., "Compressive Creep of a Lightweight, High Strength Concrete Mixture," Master of Science Thesis in Civil Engineering, Virginia Tech, January 2003.
7. Waldron, Chris, meeting in May 2003.
8. ACI Committee 209 (1990), "Prediction of creep, shrinkage and temperature effects in concrete structures." *Manual of Concrete Practice*, Part 1, 209R 1-92.
9. Huo, X. S., Al-Omaishi, N., and Tadros, M.K., Creep, Shrinkage, Modulus of Elasticity of High Performance Concrete., *ACI Materials Journal*, v. 98, n.6, November-December 2001.
10. CEB-FIP Model Code, "Evaluation of the Time Dependent Behavior of Concrete," September 1990.
11. American Association of State Highway and Transportation Officials, "AASHTO-LRFD Bridge Design Specifications," Second Edition, Washington, DC, 1998.
12. Gardner, N. J. and Lockman, M. J., "Design Provisions for Drying Shrinkage and Creep of Normal-Strength Concrete," *ACI Materials Journal*, v. 98, March-April 2001, pp. 159-167.
13. Tadros, et al. "Prestress Losses in Pretensioned High-Strength Concrete Bridge Girders," Final Report (2002).
14. Bazant, Z.P. and Baweja, S., "Creep and Shrinkage Prediction Model for Analysis and Design of Concrete Structures – Model B3," *RILEM Recommendation, Materials and Structures*, v. 28, 1995, pp. 357-365.
15. American Association of State Highway and Transportation Officials, "AASHTO-Standard Specifications for Highway Bridges," Fifteenth Edition, Washington DC (1993).